Available online at www.sciencedirect.com

ScienceDirect

journal homepage: http://www.elsevier.com/locate/rpor

Original research article

Dosimetric intercomparison of permanent Ho-166 seed's implants and HDR Ir-192 brachytherapy in breast cancer

Tarcisio Passos Ribeiro de Campos[a,*], *Luciana Batista Nogueira*[b], *Bruno Trindade*[c], *Ethel Mizrahy Cuperschmid*[d]

[a] *NRI – Nucleo de Radiações Ionizantes, Professor do Departamento de Engenharia Nuclear da Universidade Federal de Minas Gerais, Belo Horizonte, MG, Brazil*
[b] *Departamento de Anatomia e Imagem, Faculdade de Medicina, Universidade Federal de Minas Gerais, Belo Horizonte, MG, Brazil*
[c] *Programa de Ciências e Técnicas Nucleares, Núcleo de Radiações Ionizantes – NRI (Grupo de Pesquisa), UFMG, Brazil*
[d] *Centro de Memória da Medicina, Faculdade de Medicina, Universidade Federal de Minas Gerais, Brazil*

ARTICLE INFO

Article history:
Received 1 April 2015
Received in revised form
25 August 2015
Accepted 30 November 2015
Available online 4 January 2016

Keywords:
Breast brachytherapy
HDR Ir-192
Permanent implants
Ho-166 seeds
MCNP

ABSTRACT

Aim: To provide a comparative dosimetric analysis of permanent implants of Ho^{166}-seeds and temporary HDR Ir^{192}-brachytherapy through computational simulation.
Background: Brachytherapy with Ir^{192}-HDR or LDR based on temporary wires or permanent radioactive seed implants can be used as dose reinforcement for breast radiation therapy. Permanent breast implants have not been a practical clinical routine; although, I^{125} and Pd^{103}-seeds have already been reported. Biodegradable Ho^{166}-ceramic-seeds have been addressed recently.
Material and methods: Simulations of implants of nine Ho^{166}-seeds and equivalent with HDR Ir^{192}-brachytherapy were elaborated in MCNP5, shaped in a computational multivoxel simulator which reproduced a female thorax phantom. Spatial dose rate distributions and dose–volume histograms were generated. Protocol's analysis involving exposure time, seed's activities and dose were performed.
Results: Permanent Ho^{166}-seed implants presented a maximum dose rate per unit of contained activity (MDR) of 1.1601 $\mu Gy\,h^{-1}\,Bq^{-1}$; and, a normalized MDR in standard points (8 mm, equidistant to 03-seeds – SP_1, 10 mm – SP_2) of 1.0% (SP_1) and 0.5% (SP_2), respectively. Ir^{192}-brachytherapy presented MDR of 4.3945×10^{-3} $\mu Gy\,h^{-1}\,Bq^{-1}$; and, 30% (SP_1), and 20% (SP_2). Therefore, seed's implant activities of 333 MBq (Ho^{166}) and 259 GBq (Ir^{192}) produced prescribed doses of 58 Gy (SP_1; 5d) and 56 Gy (SP_1, 5 fractions, 6 min), respectively.

* *Corresponding author at*: Departamento de Engenharia Nuclear, Universidade Federal de Minas Gerais, Av. Antônio Carlos, 6627 Campus UFMG, Bloco 4, Escola de Engenharia, Belo Horizonte 31270-901, Brazil.
E-mail addresses: tprcampos@pq.cnpq.br (T.P.R. de Campos), lucibn19@yahoo.com.br (L.B. Nogueira), brmtrindade@yahoo.com (B. Trindade), ethelmizrahy@yahoo.com.br (E.M. Cuperschmid).
http://dx.doi.org/10.1016/j.rpor.2015.11.007

Conclusions: Breast Ho^{166}-implants of 37–111 MBq are attractive due to the high dose rate near 6–10 mm from seeds, equivalent to Ir^{192}-brachytherapy of 259 GBq (3 fractions, 6 min) providing similar dose in standard points at a week; however, with spatial dose distribution better confined. The seed positioning can be adjusted for controlling the breast tumor, in stages I and II, in flat and deep tumors, without any breast volumetric limitation.

1. Background

The breast cancer incidence grows at an alarming rate worldwide. Its incidence has grown annually, also in young women, reaching a factor of 10 from the 1970s to 2014. In 2015, 576,000 new cases of cancer are expected in Brazil, in which breast cancer will represent 75,000 new occurrences. Despite the diagnosis and therapy improvements, the incidence of deaths is increasing. For 57,120 new Brazilian cases of breast cancer in 2014, 13,345 deaths occurred.[1,2]

Breast conserving cancer therapy aims not only to preserve a cosmetically acceptable breast, but to diminish the recurrence of the illness.[3] If the absorbed dose produced by radiation therapy is not enough to eliminate the cancerous cell residues in the surgical tumor bed, the local recurrence will lead to radical mastectomy raising the risk for the patient and, consequently, the loss of the esthetic value of the breast. Breast conserving therapy presents cosmetic and psychological benefits for the patient and, thus, an adequate quality of life.[4,5] It is not an isolated technique, since the conserving therapy must be followed by breast radiation therapy.[6]

The radiation therapy modality often used in breast cancer is megavoltage teletherapy and cobalt therapy.[7,8] In teletherapy, the breast is irradiated in parallel opposing fields with Co-60, 4 or 6 MV LINAC, with 1.8–2.0 Gy dose fraction daily up to 5000 cGy during 5.5–6 weeks, which may be followed by a reinforcement dose in the quadrant of the tumor bed of 1000 cGy in a limited field.[9] Schemes of irradiation can also involve fields of the supraclavicular fossa, posterior axillary and internal mammary.[9,10]

Brachytherapy with Ir-192 high dose rate (HDR) or low dose rate (LDR) based on temporary Ir-192 wires or on permanent radioactive seed implants can be used as dose reinforcement for breast radiation therapy. Brachytherapy reduces the risk of local recurrence, preserves the cosmetic effect held in the conserving surgery and minimizes the early and delayed collateral effects. In Ir-192 HDR or LDR temporary Ir-192 brachytherapy, the radioactive sources, in the form of radioactive HDR segments or LDR wires, are inserted through catheters on the interstitial glandular tissue. The gamma or X-rays emissions preferentially allow the dose absorption in the surrounding volume near the tumor bed.[11]

The interstitial brachytherapy has often been used as reinforcement (boost) for the incision cavity. The protocol involves women with wide breasts, and deep tumors 4 cm beneath the skin, with unknown and positive margins microscopically and non-submitted to re-incision, or with poor pathological risk. The reason for a reinforcement dose is that such boost can complement and extend the absorbed dose provided by a conventional radiation therapy. The interstitial brachytherapy can be used as a primary method to treat the tumor bed and the adjacent tissue to the surgical excision spot.

Breast brachytherapy is safe and its results well established with long time of following up.[4,12] Brachytherapy can use multiple catheters placed in the bed of the resectable tumor, or a sole catheter where it contains on its tip a balloon that expands into the breast (Mammosite). A radioactive segment of Ir-192 of high activity, guided by a steel wire, is inserted in the catheter(s) twice a day, for 5 days, by afterloading equipment.[12] Brachytherapy is appropriate to liberate an additional reinforcement dose to the tumor bed plus margin after a standard teletherapy protocol of the entire breast. HDR Ir-192 brachytherapy uses sealed sources of 7–10 Ci, fixed in steel wires, that move into catheters and mechanical applicators previously set up on the patient. The sources are placed temporarily in the applicators. The dose distribution is generated by the repeatable process of moving-stopping actions holding the source in various internal patient's positions. The space distribution of accumulated dose is assembled in accordance with the desired organ shape, the topology of the applicator, the catheter spatial distribution, and the time of exposition. The patient typically receives a total dose in a series of daily fractions.[6]

In turn, a reinforcement protocol with Ir-192 HDR consists of 10 Gy in 2 fractions in 1 or 2 days, as example. For dose reinforcement, LDR Ir^{192} wires can also be used. The sole brachytherapy, as a primary protocol can be a choice. In this case, Ir-192 HDR applies 34 Gy, in fractions of 3.4 Gy in 10 sections, twice daily in 5 days subsequent. In terms of comparison, a primary teletherapy can provide 45–50 Gy with dose rate of 0.5 Gy h^{-1}, and reinforcement provides 15–20 Gy with 0.5 Gy h^{-1}.[13]

Permanent implants of radioactive seeds in breast cancer have not been a practical clinical routine; however, there are some studies on this matter.[14] Jakub et al., 2010, reports implants of I-125 and Pd-103 metallic seeds in breast cancer.[15,16] In turn, permanent implants of biodegradable ceramic seeds with Si, Ca and Ho composition have been developed early.[17–22] Such seeds have the length of 1.6 mm and 0.5 mm in diameter, with a polymeric resin covering. Permanent breast implants can be produced by the insertion of a set of fine hypodermic needles distributing those small seeds on the tumor. In contrast to clinical implants of metallic I-125 seeds with half-life of 59 d or HDR of Ir-192 of 74 d half-life, the Ho-166 seed implants are still in phase of in vivo experimentation.[22,23]

The holmium, with atomic number 67 and atomic mass 164.93, is of the lanthanides series – rare-earth elements,

being paramagnetic. The holmium was discovered by analysis of spectral rays, in 1878, by Jacques-Louis Soret and Marc Delafontaine and, in independent research in 1879, by Per Teodor Cleve, that provided the chemical separation of the erbium and the thulium. The Cleve researcher called the discovered element by the name of the capital of Sweden, Holmia, his home city. The Ho-165, with 100% of abundance, when submitted to a thermal and epithermal neutron surgence, produces the radioactive Ho-166 isotope by means of a nuclear reaction ^{165}Ho (n, γ) ^{166}Ho, and preferential decays by β-particle emission with 26.8 h half-life, transforming itself into the steady-state element Er-166. The maximum energy of β-particle is 1855 keV.[24,25]

The Monte Carlo technique propitiates a numerical solution for nuclear particle transport in the human body, simulating the trajectories of the particles in function of its probabilities of interaction in the multiple voxels or in the surrounding environment. The MC technique interprets the complex process of particle-atomic interactions.[26] It has been avoided to be used in the medical radiation therapy centers due to the high computational cost. MC can predict the absorbed doses generated on radiotherapy and radiology applied to human being through the direct simulation of the dynamics of nuclear particles in the subject in question. In this direction, the MC method is essentially simple and generates a macroscopic approach of the particle distribution and energies in the human body through the simulations of the electron, neutron, proton or photon microscopic interactions in the electronic and nuclear atomic level. The solution is determined by the multiple random sampling of the physical microscopic interactions between particles and target until convergence of the results occurs.[26] Deterministic fast solutions, with low computational cost, are recommended for problems of low degree of complexity; while, the Monte Carlo technique becomes advantageous in the analysis of problems with complex geometries and diversity in material and chemical composition exemplified by radiotherapic protocols applied to human beings.

SISCODES, a computational system for dosimetry of neutrons and photons by stochastic methods is a tool for preparing a computational simulator for radiation therapy. It provides an analysis of the particle transport made by stochastic codes, such as MCNP.[27,28] This system allows the conversion of a set of tomographic images creating a voxel model linked to a data base of chemical compositions of tissues and nuclear data. The SISCODES allows the association of nuclear and chemical data to each voxel through the identification of a tissue by Hounsfield number or user's election, as well as the positioning of the brachytherapy and teletherapy sources. The system uses the MCNP for the simulation of the nuclear particle transport in the model. From the results, the dosimetric data are extracted and presented by means of space dose distributions and dose versus volume histograms.[27] There were no needs to validate the SISCODES for brachytherapy photon transport, since SISCODES only generates an input file for running on MC code and manipulates its code's output. Therefore, particle-transport validation will be done on the level of MC code. However, MCNP has been already accepted for electron and photon transport found in brachytherapy.

Radioactive sealed sources are often applied on brachytherapy in order to provide a suitable spatial dose distribution in source's neighboring tissues. The required unit quantity for an Ir^{192} gamma-emission source is the reference source strength in both reference air kerma strength, S_K, given as units of $\mu Gy\,m^2\,h^{-1}$, and contained activity in Bq. Air Kerma Strength Unit, namely U, is equal to $1\,\mu Gy\,m^2\,h^{-1}$ or $1\,cGy\,cm^2\,h^{-1}$.[29] Brachytherapy source strength is specified in terms of air kerma rate at a point in air taken at the perpendicular bisector of the source segment, being the product of air kerma rate times the distance to a point, usually 1 m. Air kerma strength conversion for ^{192}Ir of $1\,\mu Gy\,m^2\,h^{-1}$ is equal to 8.991 MBq.[29–31] A conversion factor of 1.0891×10^{-5} U to 1 Bq of Ir-192 is also found. In addition, the recommended quantity for specifying a beta-emission source is the reference absorbed dose rate in water at a reference point of 2 mm from the seeds taken at the transverse direction from the source's longitudinal axis at its center. Such quantities and units are used on source specification and calibration. On the other hand, on simulations, the Monte-Carlo code provides dose per particle emitted by source. A simulated history reproduces the interactions that occurred with an electron or photon particle emitted by source up to its absorption or leakage. The number of histories will be related to contained activity by disintegration probabilities and yields addressed on the radioactive decayment. Thus, it can be mentioned that Monte-Carlo models predict dose rate per unit contained source activity in units of $cGy\,h^{-1}\,Bq$. In order to compare the predictions of a model to dose rate measurements involving two distinct emitting sources, the source in question will be addressed as contained activity. Contained activity of a beta-source may be determined by dissolving the source material in a liquid medium that holds the total contained activity enclosed in an aqueous solution. An established reference absorbed dose rate per unit activity conversion factor for a particular source is used to convert contained activity to reference absorbed dose rate. These conversion factors are generated using a combination of Monte-Carlo calculations and absorbed dose rate experimental measurements.[29–31]

2. Aims

The present article presents a dosimetric intercomparison of breast implants simulated by the radioactive sources in geometric conditions and similar spatial distribution of the permanent Ho^{166} seeds and temporary radioactive Ir-192 HDR segments. It made use of the spatial dose rate distributions normalized by the source contained activity and in an equivalent spatial point of references. The dosimetric intercomparison is possible in similar anatomy (geometry and material) and equivalent time of exposition.[23] Here, the reproduction of such equivalent conditions is achieved by computational methods so that the dosimetry produced for permanent Ho-166 seed protocol, in study, and HDR Ir-192 protocol, already established in the practical clinic, can be compared and analyzed, in a way that such conditions cannot be reached in real clinical situations.

3. Material and methods

3.1. Simulator

A computer tomography scan (CT) of a female thorax phantom[21] provided a set of images for mounting a computational breast model. The images were taken on the GE CT Healthcare. A radiotransparent support was placed on the thorax phantom, positioned in the dorsal decubitus. A current and voltage of 80 mA and 120 kV were selected, correspondent to a routine thorax CT. The scanning length was 184.5 cm, with 2.0 mm thickness, totaling 91 sections. The CT images were used for elaboration of the voxel model of the breast phantom using the SISCODES code. The model was mounted through the identification of similar gray level, correspondents to the synthetic tissues. These tissues had been identified in a database of tissues connected to SISCODES in which the chemical composition and the mass density of synthetic tissues were registered equivalents to ICRU-44.[25]

3.2. Ho-166 seed protocol

The implant simulation was performed on the voxel model of the synthetic breast of the thorax phantom.[28] The voxel dimension in X and Y was 1.87 mm and 2 mm in Z. Nine seeds of Ho-166 had been distributed, arbitrarily implanted in the left breast, in three insertions (equivalent to a triangle) each vertex receiving three seeds spaced 10 mm from each other, on the following positions (−8.0, 7.5, 5.0); (−7.15, 7.0, 5.0); (−8.0, 6.5, 5.0); (−8.0, 7.5, 4.0); (−7.15, 7.0, 4.0); (−8.0, 6.5, 4.0); (−8.0, 7.5, 3.0); (−7.15, 7.0, 3.0); (−8.0, 6.5, 3.0). The seeds of Ho-166 have active nucleus of 0.4 mm of diameter and 1.12 mm of length, coated with 0.05 mm of plastic resin. Table 1 specifies the energies of the particle emission from Ho-166 simulated on the MCNP code. A continuous spectrum of beta-particle emissions was adopted. Table 1 presents the β and γ energies of the Ho-166 radiations, respectively, including its maximum, average values and relative intensity in percentage of occurrence. Fig. 1 presents the physical and geometric structure of these Ho-166 seeds.

Table 1 – (a) X-ray and gamma emitted by Ho-166; (b) maximum and average energies of the β radiations emitted by Ho-166 [24].

Energy (keV)	Intensity (%)
80.574	6.71
184.40	0.0020
520.80	0.00033
674.00	0.0194
705.30	0.0131
785.89	0.0119
1263.08	0.0014
1379.40	0.93
1447.59	0.00098
1528.20	0.0002
1581.89	0.187
1662.48	0.120
1749.91	0.0277
1830.49	0.0085

E_{max} (keV)	E_{mean} (keV)	Yield (%)
1854.7	693.6	50.0
1773.1	650.9	48.7
1068.0	369.0	0.0061
394.0	114.9	0.95
325.7	105.1	0.0024
191.5	51.9	0.307
23.4	5.9	0.0362

3.3. Ir-192 HDR brachytherapy

The simulation used the same voxel model of the synthetic breast with the same voxel's dimensions. An Ir-192 HDR afterloading brachytherapy protocol was considered. A radioactive segment was assumed located into catheters placed in the left breast following nine similar Ho-166 seed positions holding equal exposure time in each position: (−8.0, 7.5, 5.0); (−7.15, 7.0, 5.0); (−8.0, 6.5, 5.0); (−8.0, 7.5, 4.0); (−7.15, 7.0, 4.0); (−8.0, 6.5, 4.0); (−8.0, 7.5, 3.0); (−7.15, 7.0, 3.0); (−8.0, 6.5, 3.0). The metallic linear segment of Ir-192 had an active nucleus of 1 mm of diameter and 5 mm of length, coated with 0.05 mm of steel. The emissions of Ir-192 were taken from ENDFBVI.[33]

3.4. Software

The SISCODES/MCNP computational system was used in the simulations. After the simulation of the implants on MCNP

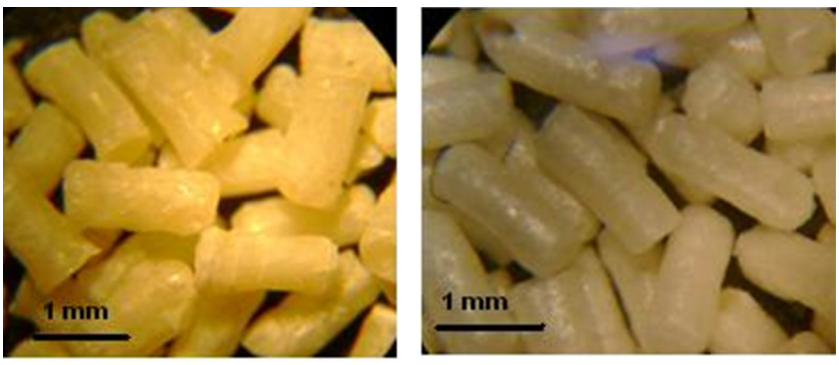

Fig. 1 – (a) Images of [Si: Ca: Ho] seeds and (b) [Si: Ca: Ho: Zr] seeds in stereoscopic image 80×.

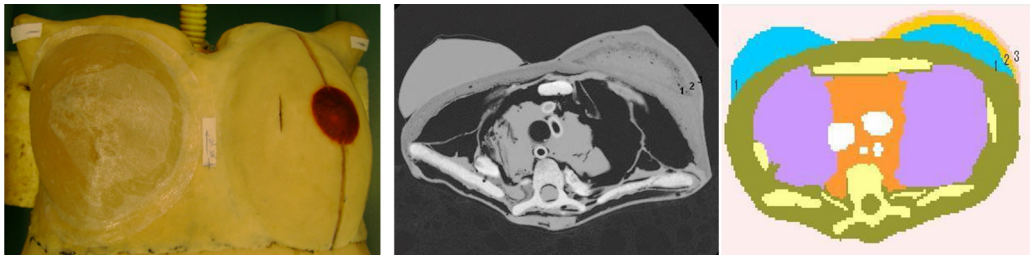

Fig. 2 – (a) Physical thorax phantom; (b) axial thorax section of the computational voxel model generated in the SISCODES interface; (c) an axial CT section of the thorax phantom.

Fig. 3 – Spatial dose rate distribution normalized in function of the contained activity of the seeds, induced by photons of the Ho-166 decayment, with MDR of 1.6756 x 10^{-3} μGy h^{-1} Bq^{-1}.

(version 5.2), the normalized values of dose rate per unit of contained activity were exported to SISCODES. Thus, the spatial dose rate distributions were generated for each procedure. The values were normalized in function of the total contained activity of the seeds. The contained activity of the seeds was calculated in order that the control point achieves a dose close to 60 Gy (equidistant of the 03 seed punctions). With this contained activity, the doses in the target region and adjacent tissues were evaluated and represented by color isodoses in intervals.

3.5. *Uncertainties*

The computational uncertainties were generated for each voxel of the model for the MCNP5 code. Those were dependents of the running particle number. The uncertainties had been kept for each voxel inferior to 5% for voxels into the mammary tissue. These values get lower in function of the proximity of the radioactive sources due to the increase of the number of events.

4. Results

The results of the computational simulations of the radiotherapy protocols reproducing the permanent implants of 09 Ho-166 seeds, in the same positions, and the linear segments of Ir-192 are presented.

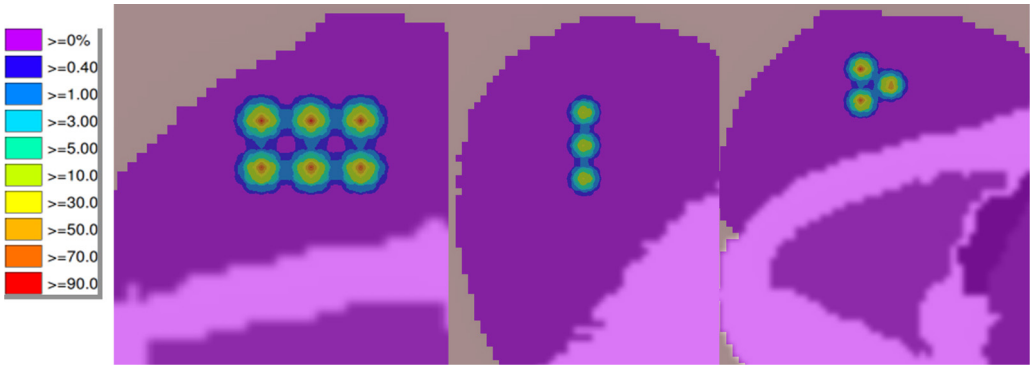

Fig. 4 – Spatial dose rate distribution normalized in function of the contained activity of the seeds, induced by electrons of the Ho-166 decayment, with MDR of 1.1585 μGy h^{-1} Bq^{-1}.

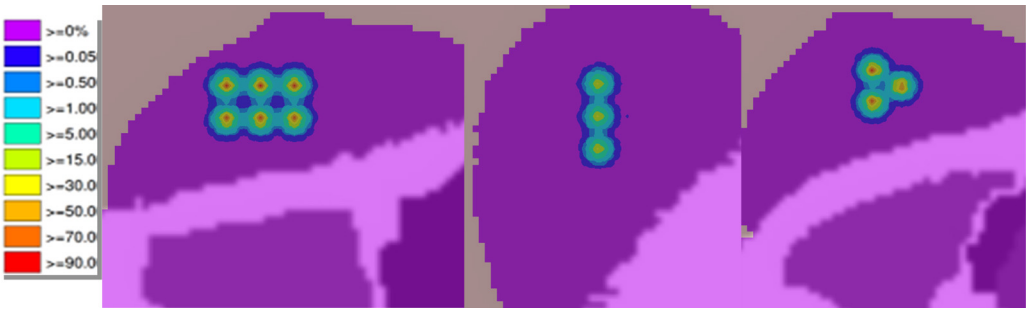

Fig. 5 – Spatial dose rate distribution normalized in function of the contained activity of the seeds, induced by electrons and photons of the Ho-166 decayment, with MDR of 1.1601 μGy h^{-1} Bq^{-1}.

4.1. *Breast computational simulator*

The breast computational simulator was reproduced mimicking the physical breast phantom. Image of the physical simulator and axial sections from the set of CT images and from its computational model are shown in Fig. 2.

The voxel model is representative of the physical thorax phantom.[32] The right breast is constituted of gelatinous tissue, homogeneous and equivalent to human glandular tissue. The simulations had been executed in the left synthetic breast. The left synthetic breast is constituted of synthetic elastomer, adipose and glandular synthetic tissues. The radiological equivalence could be evaluated in the CT images of the left breast phantom with the human breast, previously described.[32] Fig. 2 presents a section of the computational voxel model and the corresponding CT section. It is possible to distinguish three tissues: glandular (1), adipose (2) and skin (3) constituent of the phantom.

The computational voxel model of the whole breast was elaborated on the SISCODES using the set of 91 CT images generated on the female thorax phantom. Fig. 2(b) shows the voxel model of the thorax phantom in the axial section. This model was constructed in accordance with the characteristics of the constituent tissues by means of a database connected to the SISCODES code, in which defined the chemical composition and mass density of the equivalent tissue is defined. This model is useful in dosimetric studies applying the MCNP code.

4.2. *Ho-166 seed implants*

Fig. 3 illustrates the spatial dose rate distribution in function of the total contained activity of the seeds, due to the photon emitted by the radioactive Ho-166 seeds. The values were converted of MeV g^{-1} t^{-1} (t = transition) for μGy h^{-1} Bq^{-1}. Such distribution of seeds produced normalized dose rates referent to the maximum value at 100% equal to 1.6756×10^{-3} μGy h^{-1} Bq^{-1} for photon emitted by Ho-166.

Fig. 4 presents the spatial dose rate distribution normalized in function of the total contained activity of the set of seeds, in the lateral, sagittal and axial sections. These partial results are referring to electrons emitted by the continuous spectrum of the beta-decayment of the Ho-166. The units were converted of MeV t^{-1} (energy deposited in each voxel for transition) into unit of μGy h^{-1} Bq^{-1}, then divided by the weight of each voxel. The MDR value of 100% was 1.1585 μGy h^{-1} Bq^{-1} (after unit conversion). For example, the value of 0.05% represents 0.0579 μGy h^{-1} Bq^{-1}.

Fig. 5 illustrates the spatial dose rate distribution normalized in function of the contained activity of the Ho-166 seeds, summing the emissions of betas (electrons), gamma-rays and X-rays. The values had individually been evaluated in each voxel and added after being converted into the same unit of μGy h^{-1} Bq^{-1}. The maximum value of 100% was 1.1601 μGy h^{-1} Bq^{-1} in the voxel (39, 17, 20) (after unit conversion). The value of 0.05% represents 0.0580 μGy h^{-1} Bq^{-1} and occurs 9 mm from the Ho-166 seed out of the implant.

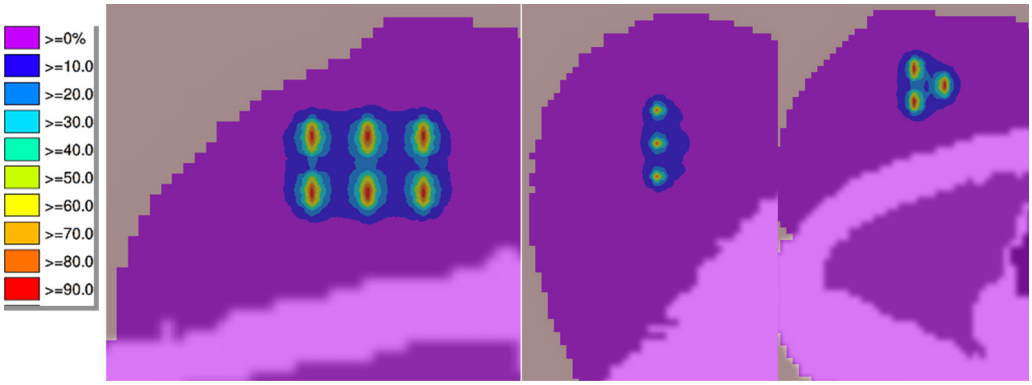

Fig. 6 – Spatial dose rate distribution normalized in function of the contained activity of the radioactive segment of Ir-192 (HDR brachytherapy) induced by photons of the Ir-192 decayment, with MDR of 4.3945×10^{-3} μGy h^{-1} Bq^{-1}.

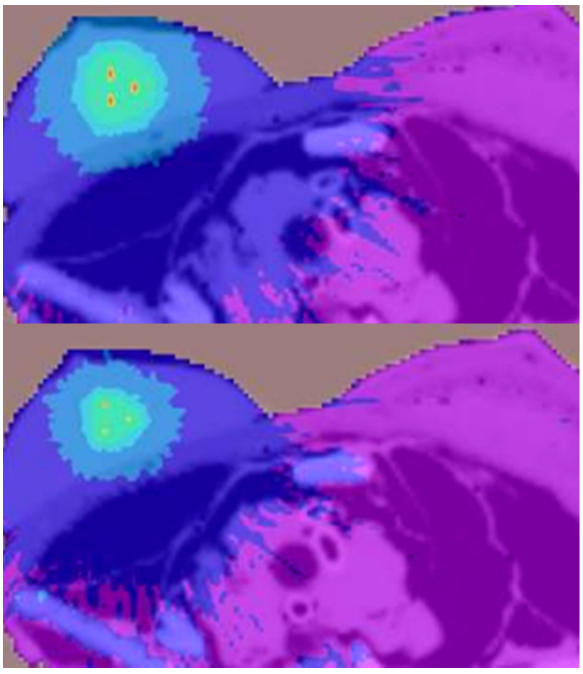

Fig. 7 – Spatial photon dose rate distribution for (a) HDR Ir-192 and (b) Ho-166 seeds at the first three color intervals (0.1,1); (1,3); (3,5) in %, normalized in function of the contained activity.

4.3. *Simulation with Ir-192 HDR*

Fig. 6 presents the spatial dose rate distribution normalized in function of the contained activity of the source distributed in the 09 equivalent positions covered for the radioactive Ir-192 segment of 259 GBq, produced in automated HDR brachytherapy, in the lateral, saggital and axial sections.

Fig. 7 depicted the dose rate distributions at 0.1 up to 5%, normalized in function of the contained activity for HDR Ir-192 and Ho-166 seeds. A larger dose rate spreading over the internal organs can be observed to HDR Ir-192 in relation to the Ho-166 distribution. Also, the dose rate values for Ho-166 were 40% lower than HDR Ir-192, on this interval (Fig. 7).

4.4. *DVH histograms*

The dose-volume histograms at the lung, skin, fibroglandular and adipose breast tissues for Ho-166 seed implants and HDR Ir^{192} brachytherapy, based on equivalent physical and geometric simulation conditions, are presented in Fig. 8. The histogram demonstrates that the Ho-166 seed's implant provides an absorbed dose more confined on the implant's volume than the HDR Ir^{192} brachytherapy. Such results are relevant especially to skin and lung tissues.

5. Discussion

Table 2 presents values of the accumulated total dose evaluated on the simulations of the two protocols. The protocol of permanent implant of nine seeds of Ho-166 [Si: Ca: Ho]

Table 2 – Dosimetric intercomparison of the radiotherapy breast protocols.

Protocol[d]	Dimens. [mm]	MDR_{100}[e] $\mu Gy\,h^{-1}\,Bq^{-1}$	FD in PR[c] [%]	PR[b] [mm]	A_T[f] [MBq]	T (n[f]) [h]	Nucl.	$T_{1/2}$[f] [h]	FA[d] [h]	$(D_F)D_T$[f] [Gy]
[Ho:Si:Ca][a]	1.6 × 0.5	1.1601 (β ± γ) 1.6756 × 10^{-3} (γ); 1.1585 (β)	0.4–1.0	8–6	333	∝	Ho^{166}	26.8	37.5	58/145
HDR-Ir^{192}	5 × 1	4.3945 × 10^{-3} (γ)	10–20	8–6	259,000	0.1 (5)	Ir^{192}	1772	0.0999	(11.37) 57/68

Notes: A_T = total contained activity in the implant; D_F = dose per fraction in the T time (in case of temporary implant); D_T = accumulated total dose; $T_{1/2}$ = half-live of nuclide.

[a] Permanent implants of interstitial biodegradable ceramic seeds for 03 punctions, with 03 inserted seeds in AWG12 needles, equidistant of 10 mm each, having distributed 09 total seeds.

[b] PR = position of reference equidistant 6 mm of the three punctions.

[c] FD = dose factor in PR, representing the percentile of the maximum dose rate (MDR) in the position at the spatial dose rate distribution generated in the simulation.

[d] FA = factor of accumulation, $(1 - \exp(\lambda T))/\lambda$, where λ is the decay constant and T the exposition time.

[e] MDR_{100} = dose rate at 100% in unit of $\mu Gy\,h^{-1}\,Bq^{-1}$.

[f] n number of fractions, in fractionate case.

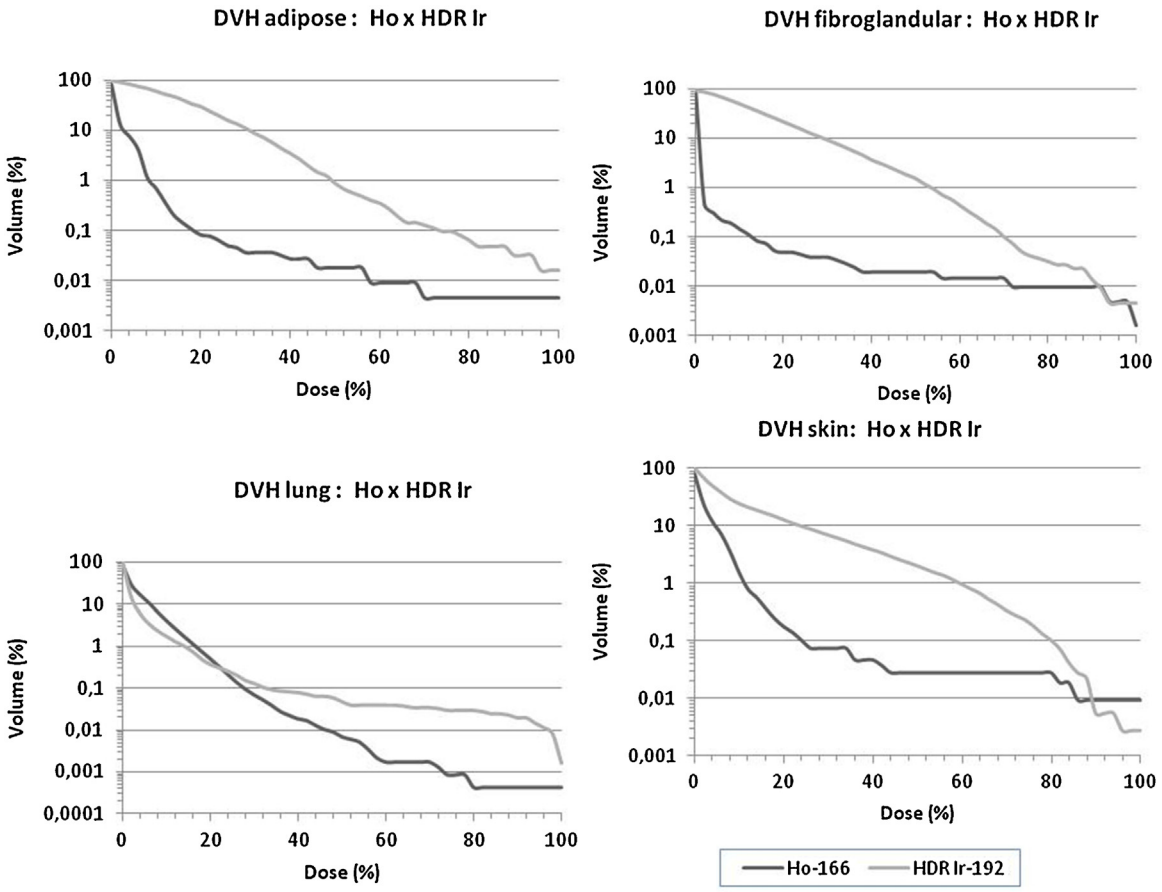

Fig. 8 – Dose-volume histograms at the lung, skin, fibroglandular and adipose breast tissues for Ho-166 seed implants and HDR Ir^{192} brachytherapy, based on equivalent physical and geometric conditions.

produced an accumulated total dose of 58 Gy at the control point, equidistant to the three punctions (6–8 mm) each being punction with a set of 03 seeds. Positions next to the seeds have higher dose values. The total dose produced by the implant is superior to the prescribed dose provided by radiotherapy as megavoltage teletherapy of 25 fractions of 200 cGy, being also superior to a dose of reinforcement as 10–15 Gy. However, it was limited to the implant volume and it was not distributed over the whole glandular tissue as provided by the teletherapy of 6 MV with two parallel opposing fields of 10 cm × 10 cm. The spatial dose rate distribution at the permanent implant of Ho-166 seeds showed that the dose accumulates into the defined volume of the implant, preserving the lung at the distance of a few centimeters. The uncertainties of the doses calculated by the computational model, in voxels into the implant volume are in order of 0.5–1.0%. These uncertainties increase toward out the implant rising from 1.0 up to 5.0%; however, such voxels are irrelevant for this analysis whose doses are lower than 0.001% MDR.

The dosimetric intercomparison of HDR Ir-192 brachytherapy of 259 GBq and the permanent implantation of Ho-166 seeds at the same source positioning showed high doses confined to the implant volume, and demonstrated that both are of high rate. For example, in the central point of the implant (control point – 6 mm equidistant) HDR Ir-192 produces 113.75 Gy h^{-1} with 259 GBq; while the seeds of Ho-166 produce 1.55 Gy h^{-1} with seed's contained activity of 74 MBq. HDR Ir-192 brachytherapy is temporary and occurs in the 10 fractions of 6–10 min, as example, which allows a time factor of accumulation of 0.0999–0.1699. The Ho-166 seeds are implanted permanently; however, due to half-life of 26 h, the total dose is also deposited in one week, with a time factor of accumulation over 37.51 at 5 days. It was an option on this study making use of a set of nine seeds to compose an irradiated volume holding it sufficiently limited. The present situation mimics tumors in initial staging, in situ, resectable or not.

6. Conclusions

Protocols of implants of Ho-166 ceramic seeds for breast radiation therapy are attractive due to their high dose rate equivalent to Ir-192 HDR brachytherapy, providing possible similar accumulative dose in reference's points; however, with spatial dose distribution confined into the implant volume. Both treatments can be accomplished in one week. The permanent Ho^{166} seed implant produces a profile of high doses in limited volume, predefined in accordance with the distribution of the seeds. The three-dimensional dose profile can

be adjusted for controlling the breast tumors, in I and II stage, being able to be used on tumors located 02 cm from the skin or deeper, without breast volume limitation. The seeds must be distributed on the tumor volume or at the tumor bed, spaced maximum 10 mm apart.

Conflict of interest

None declared.

Financial disclosure

None declared.

Acknowledgements

The authors are thankful to the financial support of the Conselho Nacional de Desenvolvimento da Pesquisa – CNPq [456719/2013-0 REBRAT-SUS]; Fundação de Pesquisa do Estado de Minas Gerais – FAPEMIG – Universal [FAPEMIG – 18565 FAPEMIG] and Coordenação de Aperfeiçoamento de Pessoal de Nível Superior – CAPES for the scholarships.

REFERENCES

1. INCA. *Estimated 2014 incidence of cancer in Brazil*. Rio de Janeiro: Cancer National Institute, Ministry of Health (MH), INCA; 2014.
2. IARC. *Globocan 2012, Estimated cancer incidence, mortality and prevalence worldwide in 2012*. International Agency for Research on Cancer, World Health Organization; 2012. http://globocan.iarc.fr [accessed June, 2014].
3. Tiezzi DG. Cirurgia conservadora no câncer de mama [Breast-conserving surgery for breast cancer]. *Rev Bras Ginecol Obstet* 2007;**29**(8):428–34.
4. Grace LS, Jing J, Thomas AB, et al. Benefit of adjuvant brachytherapy versus external beam radiation for early breast cancer: impact of patient stratification on breast preservation. *Int J Radiat Oncol Biol Phys* 2014;**88**(2):274–84.
5. Halperin EC, Brady LW, Perez CA, Wazer DE. *Principles and practice of radiation oncology*. 6th ed. Lippincott Williams & Wilkins; 2008.
6. Perez CA, Taylor ME, Halverson K, Garcia D, Kusm RR, Locmr MA. Brachytherapy or electron beam boost in conservation therapy of carcinoma of the breast: a nonrandomized comparison. *J Radiation Oncol Biol Phys* 1996;**34**(5): 995–1007.
7. Clarke DH, Edmundson GK, Martinez AA, Matter RC, Warmelink C. The utilization of I-125 seeds as a substitute for Ir-192 seeds in temporary interstitial implants: an overview and description of the William Beaumont Hospital technique. *Int J Radiat Oncol Biol Phys* 1998;**15**:1027–33.
8. Zelefsky MJ, Valicenti RK, Hunt M, Perez CA. Low risk prostate cancer. In: Halperin EC, Perez CA, Brady LW, editors. *Principles and practice of radiation oncology*, 62, 5th ed. Lippincott Williams & Wilkins; 2008. p. 1440–83.
9. Faiz MK. *The physics of radiation therapy*. 4th ed; 2009. ISBN 1:0781788560.
10. Luiz AMS. *Física da Radioterapia*. São Paulo: Sarvier; 1997.
11. Purdy JA. Three-dimensional physics and treatment planning. In: Perez CA, Brady LW, editors. *Principles and practice of radiation oncology*. 3rd ed. Philadelphia: Lippincott–Raven; 1998. p. 343–70.
12. Ko ECK, Koprowskiemail CD, Dickson-Witmer D, et al. Partial vs. whole breast irradiation in a community hospital: a retrospective cohort analysis of 200 patients. *Brachytherapy* 2010;**9**(3):248–53.
13. Wazer D, Arthur DW, Vicini FV. *Accelerated partial breast irradiation: techniques and clinical implementation*. Springer-Verlag; 2006.
14. Keller B, Sankreacha R, Rakovitch E, O'brien P, Pignol JP. A permanent breast seed implant as partial breast radiation therapy for early-stage patients: a comparison of palladium-103 and iodine-125 isotopes based on radiation safety considerations. *J Radiat Oncol Biol Phys* 2005;**62**(2):358–65.
15. Jakub JW, Gray RJ, Degnim AC, Boughey JC, Gardner M, Cox CE. Current status of radioactive seed for localization of non-palpable breast lesions. *Am J Surg* 2010;**199**: 522–8.
16. *BMI, iodine-125 and palladium-103 seeds brochure*. Best Medical International Inc.; 2008.
17. Valente ES, Campos TPR. Gamma spectrometry and chemical characterization of ceramic seeds with samarium-153 and holmium-166 for brachytherapy proposal. *Appl Radiat Isot* 2010;**68**:2157–62.
18. Valente ES, Cuperschmid EM, Campos TPR. Evaluation of HeLa cell lineage response to beta radiation from holmium-166 embedded in ceramic seeds. *Braz Arch Biol Technol* 2011;**54**:957–64.
19. Nogueira LB, Campos TPR. Nuclear characterization and investigation of radioactive bioglass seed surfaces for brachytherapy via scanning electron microscopy. *J Sol-Gel Sci Technol* 2011;**58**:251–8.
20. Nogueira LB, Campos TPR. Radiological response of ceramics and polymeric devices for breast brachytherapy. *Int J Appl Radiat Isot* 2012;**70**:663–9.
21. Nogueira LB, Silva HLL, Campos TPR. Experimental dosimetry in conformal breast teletherapy compared with the planning system. *Appl Radiat Isot* 2015;**97**:93–100.
22. Campos TPR, Andrade JPL, Costa IT, Teixeira CH. A radioactive seed implant on a rabbit's liver following a voxel model representation for dosimetric proposals. In: *2005 International Atlantic Conference – INAC 2005*. 2005.
23. Campos TPR. Computational Simulations in Medical Radiation A New Approach to Improve Therapy Boletim da Sociedade Brasileira de Matemática (Cessou em 2001. Cont. ISSN 16787544). Rio de Janeiro. *Bull Braz Math Soc* 2006;**2**(2):720.
24. NNDC NUDAT data http://www.nndc.bnl.gov/nudat2/decaysearchdirect.jsp?nuc=166Ho&unc=nds [accessed 19.11.12].
25. ICRU 44. *Tissue substitutes in radiation dosimetry and measurement. International commission on radiation units and measurements report 44*. Bethesda, MD: ICRU; 1989.
26. Kalos MH, Whitlock PA. Monte Carlo methods. *Basics*, vol. I. New York: John Wiley & Sons; 1986.
27. Trindade BM, Campos TPR. Sistema computacional para dosimetria de nêutrons e fótons baseado em métodos estocásticos aplicados a radioterapia e radiologia. *Radiol Bras* 2011;**44**(2):109–16.
28. Campos TPR, Thompson L, Nogueira LB, Duarte IL, Matos AS, Teixeira CH, et al. (inventors). Anthropomorphic and anthropometric simulators of the structures, tissues and organs of the human body. Brazil, Patent BR PI1004465-5; May 8, 2012.
29. *Calibration of photon and beta ray sources used in brachytherapy. IAEA-TECDOC-1274*; March 2002.

30. Rivard MJ, Coursey BM, DeWerd LA, et al. Update of AAPM Task Group No 43 report. A revised AAPM protocol for brachytherapy dose calculations. *Med Phys* 2004;**31**:633–74.
31. Chandola RM, Samit Tiwari S, Kowar MK, Choudhary V. Monte Carlo and experimental dosimetric study of the mHDR-v2 brachytherapy source. *J Cancer Res Ther* 2010;**6**(4):421–6.
32. MCNP5 Monte Carlo Team. *A general Monte Carlo n-particle transport code manual version* 5. Los Alamos National Laboratory; 2003.
33. ENDF/BVI Decay Data. http://t2.lanl.gov/data/decayd.html [accessed 15.11.13].